doi:10.1093/brain/awr198 Brain 2011: 134; 2565–2581 | 2565

BRAIN
A JOURNAL OF NEUROLOGY

Clinical and neuroanatomical signatures of tissue pathology in frontotemporal lobar degeneration

Jonathan D. Rohrer,[1] Tammaryn Lashley,[2] Jonathan M. Schott,[1] Jane E. Warren,[3] Simon Mead,[4] Adrian M. Isaacs,[4] Jonathan Beck,[4] John Hardy,[5] Rohan de Silva,[5] Elizabeth Warrington,[1] Claire Troakes,[6] Safa Al-Sarraj,[7] Andrew King,[7] Barbara Borroni,[8] Matthew J. Clarkson,[1,9] Sebastien Ourselin,[1,9] Janice L. Holton,[2] Nick C. Fox,[1] Tamas Revesz,[2] Martin N. Rossor[1] and Jason D. Warren[1]

1 Dementia Research Centre, Department of Neurodegenerative Disease, UCL, Institute of Neurology, Queen Square, London WC1N 3BG, UK
2 Queen Square Brain Bank, Department of Molecular Neuroscience, UCL Institute of Neurology, London, WC1N 3BG, UK
3 Computational, Cognitive and Clinical Neuroimaging Laboratory, Imperial College London, London, W12 0NN, UK
4 MRC Prion Unit, Department of Neurodegenerative Disease, UCL Institute of Neurology, London, WC1N 3BG, UK
5 Reta Lila Weston Institute, UCL Institute of Neurology, University College London, Queen Square, London, WC1N 3BG, UK
6 MRC Centre for Neurodegeneration Research, Institute of Psychiatry, King's College London, London, SE5 8AF, UK
7 Department of Clinical Neuropathology, King's College Hospital NHS Trust, London, SE5 9RS, UK
8 The Centre for Neurodegenerative Disorders, University of Brescia, Brescia 25125, Italy
9 Centre for Medical Image Computing, Department of Medical Physics and Bioengineering, The Engineering Front Building, University College London, London, WC1E 6BT, UK

Correspondence to: Dr Jason Warren,
Dementia Research Centre,
UCL Institute of Neurology,
Queen Square,
London WC1N 3BG, UK
E-mail: jwarren@drc.ion.ucl.ac.uk

Relating clinical symptoms to neuroanatomical profiles of brain damage and ultimately to tissue pathology is a key challenge in the field of neurodegenerative disease and particularly relevant to the heterogeneous disorders that comprise the frontotemporal lobar degeneration spectrum. Here we present a retrospective analysis of clinical, neuropsychological and neuroimaging (volumetric and voxel-based morphometric) features in a pathologically ascertained cohort of 95 cases of frontotemporal lobar degeneration classified according to contemporary neuropathological criteria. Forty-eight cases (51%) had TDP-43 pathology, 42 (44%) had tau pathology and five (5%) had fused-in-sarcoma pathology. Certain relatively specific clinicopathological associations were identified. Semantic dementia was predominantly associated with TDP-43 type C pathology; frontotemporal dementia and motoneuron disease with TDP-43 type B pathology; young-onset behavioural variant frontotemporal dementia with FUS pathology; and the progressive supranuclear palsy syndrome with progressive supranuclear palsy pathology. Progressive non-fluent aphasia was most commonly associated with tau pathology. However, the most common clinical syndrome (behavioural variant frontotemporal dementia) was pathologically heterogeneous; while pathologically proven Pick's disease and corticobasal degeneration were clinically heterogeneous, and TDP-43 type A pathology was associated with similar clinical features in cases with and without progranulin mutations. Volumetric magnetic resonance imaging, voxel-based morphometry and cluster analyses of the pathological groups here suggested a neuroanatomical framework underpinning this clinical and pathological diversity. Frontotemporal lobar degeneration-associated pathologies segregated based on their cerebral atrophy profiles, according to the following scheme: asymmetric, relatively localized (predominantly temporal lobe) atrophy (TDP-43 type C); relatively symmetric, relatively localized (predominantly temporal lobe) atrophy (microtubule-associated protein tau

Received May 8, 2011. Revised July 5, 2011. Accepted July 8, 2011
© The Author (2011). Published by Oxford University Press on behalf of the Guarantors of Brain.
This is an Open Access article distributed under the terms of the Creative Commons Attribution Non-Commercial License (http://creativecommons.org/licenses/by-nc/2.5), which permits unrestricted non-commercial use, distribution, and reproduction in any medium, provided the original work is properly cited.

Downloaded from https://academic.oup.com/brain/article/134/9/2565/419546 by guest on 23 April 2025

mutations); strongly asymmetric, distributed atrophy (Pick's disease); relatively symmetric, predominantly extratemporal atrophy (corticobasal degeneration, fused-in-sarcoma pathology). TDP-43 type A pathology was associated with substantial individual variation; however, within this group progranulin mutations were associated with strongly asymmetric, distributed hemispheric atrophy. We interpret the findings in terms of emerging network models of neurodegenerative disease: the neuroanatomical specificity of particular frontotemporal lobar degeneration pathologies may depend on an interaction of disease-specific and network-specific factors.

Keywords: frontotemporal dementia; frontotemporal lobar degeneration; voxel-based morphometry; MRI; neural network

Abbreviations: FTD = frontotemporal dementia; FTLD = frontotemporal lobar degeneration; FTLD-U = FTLD with ubiquitin-positive inclusions; MND = motoneuron disease; PNFA = progressive non-fluent aphasia

Introduction

A central and difficult issue in the neurodegenerative brain diseases concerns the correspondence between phenotypic features and microscopic and molecular pathology (Weintraub and Mesulam, 2009). This issue has important implications for understanding disease neurobiology, for clinical diagnosis, and ultimately, for development and rational use of disease-modifying therapies. Such considerations are particularly pertinent to frontotemporal lobar degeneration (FTLD): a genetically and pathologically heterogeneous group of disorders that collectively constitute a common cause of dementia, particularly in younger age groups (Cairns *et al.,* 2007*a*; Mackenzie *et al.,* 2010). FTLD is a macro-anatomical descriptive term referring to the relatively selective atrophy of frontal and temporal lobes that characterizes most cases. This atrophy is underpinned by diverse pathological processes; these can be broadly classified according to the major constituents of the cellular inclusions present [tau, TAR DNA-binding protein 43 (TDP-43) or fused-in-sarcoma (FUS) protein, designated FTLD-tau, FTLD-TDP or FTLD-FUS, respectively: Mackenzie *et al.,* 2010]. A number of causative genes have been identified, of which the genes coding microtubule-associated protein tau (*MAPT*) and progranulin (*GRN*) are numerically the most important. Three canonical clinical syndromes of FTLD are described: behavioural variant frontotemporal dementia (FTD) and two language variants, semantic dementia and progressive non-fluent aphasia (PNFA). These syndromes overlap clinically with motoneuron disease (FTD-MND), corticobasal syndrome and progressive supranuclear palsy syndrome (Neary *et al.,* 1998; Seelaar *et al.,* 2011). There is a broad correspondence between canonical FTLD clinical syndromes and profiles of brain atrophy detected *in vivo* using techniques such as MRI: behavioural variant FTD is associated with atrophy predominantly involving the frontal, insula, anterior cingulate and anterior temporal lobes (especially in the non-dominant hemisphere); semantic dementia, with asymmetric atrophy predominantly involving the anterior inferior temporal lobes; and PNFA, with asymmetric (predominantly dominant hemisphere) atrophy involving anterior peri-Sylvian cortices (Seelaar *et al.,* 2011).

The distinctive, focal nature of the clinico-anatomical entities that comprise the FTLD spectrum has been recognized for many years, most notably in the seminal clinical and macro-anatomical descriptions of Arnold Pick (e.g. Pick, 1892) and early recognition of a distinctive histopathological substrate with compact, often rounded argyrophilic neuronal inclusions, which were subsequently designated as 'Pick bodies' (Alzheimer, 1911). A resurgence of interest in these disorders was heralded by Mesulam's (1982) description of primary progressive aphasias, leading to an intense international research effort devoted to FTLD and its brain correlates using a range of neuropsychological, neuroimaging and neuropathological approaches. It has recently been shown that syndromes within the FTLD spectrum map onto large-scale brain networks (Seeley *et al.,* 2009), suggesting a new paradigm for explaining the distributed and heterogeneous patterns of regional atrophy in FTLD. Following this paradigm, the macroscopic topography of network disintegration in FTLD directs the development of clinical symptoms. However, no clinico-anatomical formulation has been shown reliably to predict tissue pathology across the FTLD spectrum (Weintraub and Mesulam, 2009), leading to suggestions that the diseases constitute an overlapping complex with a collectively limited and convergent phenotypic repertoire (Kertesz, 2010). A more fundamental problem concerns the basis for phenotypic selectivity and regional neuronal vulnerability in FTLD, as in other dementias (Seeley *et al.,* 2008, 2009; Weintraub and Mesulam, 2009). Recent work in both sporadic and genetically mediated forms of FTLD has suggested potential micro-anatomical (Seeley *et al.,* 2006) and molecular (Rohrer *et al.,* 2010*b*, *e*) bases for distinctive phenotypic features within the FTLD spectrum. Furthermore, recent advances in immunophenotyping have transformed and expanded our histopathological picture of FTLD (Mackenzie *et al.,* 2010).

The normal brain contains six isoforms of tau, with either three (3R-tau) or four (4R-tau) microtubule-binding repeats. Mutations of the *MAPT* gene are associated with two patterns of abnormal tau accumulation: mutations in the coding region outside exon 10 lead to accumulation of both 3R- and 4R-tau restricted to neurons, while mutations in the coding region of exon 10 (or with increased splicing of exon 10) lead to accumulation of 4R-tau in both neurons and glia. Most sporadic tauopathies (including corticobasal degeneration and progressive supranuclear palsy) have predominant 4R-tau deposition (Sergeant *et al.,* 1999); however, Pick bodies contain predominantly or exclusively 3R-tau (de Silva *et al.,* 2006). In this article, corticobasal degeneration and progressive supranuclear palsy are used to refer to the pathological entities corticobasal degeneration and progressive supranuclear palsy, distinguished from the clinical designations of

Downloaded from https://academic.oup.com/brain/article/134/9/2565/419546 by guest on 23 April 2025

corticobasal syndrome and progressive supranuclear palsy syndrome. The classification of non-tau FTLD pathologies continues to be refined. Two nomenclature systems subtyping FTLD-TDP based on detailed immunohistochemical and morphological analysis are currently in use (Mackenzie *et al.,* 2006; Sampathu *et al.,* 2006); recently, a scheme for harmonizing these two pathological classification systems was proposed (Mackenzie *et al.,* 2011), and has been adopted here. Four subtypes of FTLD-TDP have been described: type A (TDP-A), associated in a proportion of cases with mutations in the *GRN* gene; type B (TDP-B), associated with FTD-MND; type C (TDP-C) associated predominantly with semantic dementia; and type D (TDP-D), associated with mutations in the valosin-containing protein (*VCP*) gene (Mackenzie *et al.,* 2010). Several pathological entities within the non-tau spectrum but lacking TDP-43 [including cases previously described as atypical FTLD with ubiquitin-positive inclusions (FTLD-U), neuronal intermediate filament inclusion disease and basophilic inclusion body disease] have recently been shown to have predominant accumulation of FUS protein (FTLD-FUS; Munoz *et al.,* 2009; Neumann *et al.,* 2009*a*, *b*; Urwin *et al.,* 2010; Lashley *et al.,* 2011). Finally, a small proportion of cases of FTLD have inclusions negative for tau, TDP-43 or FUS, including cases associated with charged multivesicular body protein 2B (*CHMP2B*) mutations (ubiquitin-positive, TDP-43- and FUS-negative inclusions: FTLD-UPS) and others lacking inclusions (Mackenzie *et al.,* 2010). This capacity for enhanced immunohistochemical and molecular differentiation of FTLD provides an unprecedented opportunity to assess phenotypic associations within the FTLD spectrum that may previously have been obscure.

Here we undertook a detailed analysis of clinical, neuropsychological and neuroimaging features in a large retrospectively ascertained series of patients with pathologically confirmed FTLD attending a tertiary cognitive disorders clinic. Cases were characterized using a uniform neuropathological protocol motivated by recent advances in immunohistochemical and genetic diagnoses. We used the complementary techniques of magnetic resonance volumetry and voxel-based morphometry to assess neuroanatomical associations of pathologically and genetically characterized disease groups. Our objectives were to identify clinical and neuroanatomical signatures of FTLD pathologies, as defined using contemporary histopathological and molecular techniques; and to interpret such signatures in light of the emerging paradigm of network-mediated neurodegeneration in FTLD. Our central hypotheses were first, that molecular pathologies of FTLD translate to identifiable profiles of large-scale brain network damage; and secondly, that these profiles show specificity for particular FTLD pathologies.

Materials and methods

We retrospectively reviewed the database of the Specialist Cognitive Disorders Clinic at the National Hospital for Neurology and Neurosurgery, Queen Square, London, UK for the period 1993–2009 in order to identify patients with a pathological diagnosis within the FTLD spectrum (Cairns *et al.,* 2007; Mackenzie *et al.,* 2010). Ninety-five patients were identified (90 with post-mortem; 5 with *in vivo* diagnostic frontal lobe biopsy confirmation). All pathological specimens were assessed using a standard protocol and genetic, demographic, clinical, neuropsychological and neuroimaging data were analysed. Ethical approval for the study was obtained from the National Hospital for Neurology and Neurosurgery Local Research Ethics Committee.

Neuropathological and genetic analyses

Brain specimens were obtained from the Queen Square Brain Bank, London and the Institute of Psychiatry, London. The samples were fixed in 10% buffered formalin for histopathology and immunohistochemistry. Histological sections of representative brain regions of the 90 post-mortem cases and the five frontal cortical biopsies were stained with haematoxylin and eosin. Immunohistochemistry was performed using a panel of antibodies. Anti-tau antibodies comprised the AT8 monoclonal antibody against tau phosphorylated at Ser 202/Thr 205 (1 : 600, Autogen Bioclear); RD3 against 3R-tau (1 : 10 000, Upstate) and RD4 monoclonal antibody against 4R-tau (1 : 100, Upstate). A primary antibody was applied recognizing the TDP-43 protein at amino acids 1–261 (1 : 800, Abnova). FUS pathology was recognized using the anti-FUS antibody to amino acids 1–50 (1 : 200, Novus). In addition, antibodies to ubiquitin (1 : 200, Dako), p62 (1 : 200, BD Transduction Laboratories), α-synuclein (1 : 50, Vector), Aβ (1 : 100, Dako) and GFAP (1 : 1000, Dako) were used. After the primary antibody was applied sections were incubated with a biotinylated anti-mouse (1 : 200, Dako) or anti-rabbit (1 : 200, Dako) secondary antibody, as appropriate. Finally, ABC (Dako) was applied and colour was developed by diaminobenzidine/H_2O_2. The neuropathological diagnosis was determined using established diagnostic criteria, in line with consensus recommendations for the FTLD spectrum and for specific entities within the spectrum (Cairns *et al.,* 2007; Mackenzie *et al.,* 2009, 2010; Munoz *et al.,* 2009; Neumann *et al.,* 2009*a*, *b*). Details of histopathological findings are summarized in the Supplementary Material.

For all post-mortem cases, additional (non-FTLD) pathological features were determined and quantified according to standard criteria. Quantitation of Aβ-positive mature and diffuse plaques was performed based on Consortium to Establish a Registry for Alzheimer's Disease (CERAD) recommendations (Lashley *et al.,* 2008). Alzheimer-type neurofibrillary tangle pathology was determined using AT8 immunohistochemistry for Braak staging (Braak *et al.,* 2006). The extent and severity of cerebral amyloid angiopathy was determined based on a four-tier grading system (Olichney *et al.*, 1996; Lashley *et al.,* 2008). The presence of cerebrovascular pathology was examined in the frontal lobe, basal ganglia and pons using a previously described approach (Williams *et al.,* 2007). This included atherosclerosis, lipohyalinosis, micro-aneurysm and arteriolosclerosis and their sequelae, such as lacunes and perivascular rarefaction. Vascular pathology was graded as mild (occasional vessels affected), moderate (a significant proportion of the small vessels affected with few or no sequelae noted) or severe (a significant proportion of the small vessels affected with obvious sequelae).

All patients with available DNA ($n = 71$) were screened for known mutations in progranulin (*GRN*), microtubule-associated protein tau (*MAPT*), valosin-containing protein (*VCP*), fused-in-sarcoma (*FUS*), TAR DNA-binding protein (*TARDP*) and charged multivesicular body protein 2B (*CHMP2B*) genes as part of a previous study (for details see Rohrer *et al.,* 2009). The *GRN* 3′ untranslated region rs5848 genotype, reported as a risk factor for FTLD-TDP (Rademakers *et al.,* 2008) had also been assessed in all cases with DNA as part of a previous study (Rollinson *et al.,* 2011).

Downloaded from https://academic.oup.com/brain/article/134/9/2565/419546 by guest on 23 April 2025

Clinical and neuropsychological analysis

Clinical diagnosis in each patient was based upon a structured review of the clinical history and examination findings as recorded in the case file. Consensus criteria were followed (Litvan *et al.,* 1996; Neary *et al.,* 1998; Boeve *et al.,* 2003). Neuropsychological assessments were reviewed and data extracted for relevant cognitive measures (Supplementary Material).

Neuroimaging analysis: volumetric data

Forty-two patients [26 males, mean age at scan 60.0 (SD 8.8) years] had volumetric magnetic resonance brain imaging performed on a 1.5T GE Signa scanner (General Electric). Magnetic resonance brain images were also acquired for 35 age-matched cognitively normal control subjects [16 males, mean age at scan 63.7 (SD 7.0) years]. Whole brain and cerebral hemisphere volumes were calculated in all individuals as previously described (Rohrer *et al.,* 2010*e*), and an index of cerebral asymmetry was derived [(absolute hemispheric volume difference/whole brain volume × 100)]. Volumetric analysis of grey matter cortical and subcortical (hippocampus, amygdala, caudate, putamen and brainstem) areas was performed using the Freesurfer image analysis suite (version 4.0.3; http://surfer.nmr.mgh.harvard.edu/), on a 64-bit Linux CentOS 4 Sun Grid Engine Cluster. These brain regions were selected on the basis they were likely *a priori* to be targeted by pathologies in the FTLD spectrum.

Regional volumetric data for each patient were analysed statistically using STATA 10.0 (Stata Corporation). Individual regional brain sub-volumes were calculated as the mean of left and right volume values for each region and corrected for total intracranial volume. Linear regression with 95% bias-corrected bootstrap confidence intervals and 1000 replicates was used to assess for differences in total intracranial volume-corrected brain sub-volumes between disease groups and controls, and between disease groups. Logistic regression was used to explore associations between neuroimaging parameters and pathological diagnosis. Each pathological diagnosis with available MRI data was assessed in turn and the relationship of each diagnosis with regional brain volumes and with cerebral asymmetry index was compared with all other pathological diagnoses. For each diagnostic group, parameters showing significant differences ($P < 0.05$) in univariate analyses were then entered into a multivariate reverse stepwise model.

Neuroimaging analysis: group-level voxel morphometry data

Voxel-based morphometry was undertaken to assess group-level changes associated with pathological diagnoses relative to the healthy control group. Brain images were entered into the voxel-based morphometry analysis using SPM5 software (http://www.fil.ion.ucl.ac.uk/spm) and the DARTEL toolbox, and grey and white matter brain segments were derived as previously described (Rohrer *et al.,* 2010*d*, *e*). Voxel-based morphometry is an unbiased technique that makes no prior assumptions about the distribution of atrophy in particular diseases; it can therefore be regarded as complementary to regional volumetry. In order to capture individual hemispheric asymmetries that might otherwise be obscured in a group voxel-based morphometry analysis after mapping all brain images into a common space, we performed the analysis on images flipped from native space in the midsagittal plane within SPM5, such that the most severely affected cerebral hemisphere was on the same side in each patient. This procedure ensured that any group-level asymmetry of atrophy (whether atrophy was predominantly left- or right-ward directed in individual subjects) would be evident in the group analysis. An individual image was selected for flipping if it had a hemispheric asymmetry index outside the control range and more severe right hemisphere atrophy (i.e. images were flipped such that any asymmetric atrophy was displayed on the left). Voxel intensity was modelled as a function of group membership, and subject age, gender and total intracranial volume were included as nuisance covariates. Separate analyses were performed on the grey matter and white matter segments. Statistical parametric maps were generated showing significant differences between each pathological group and the healthy control group; these *t*-statistic maps were thresholded at significance level 0.01 (corrected for multiple comparisons over the whole brain volume using false discovery rate). Maps were displayed as overlays on a study-specific template brain image, created by warping all native space whole-brain images to the final DARTEL template and calculating the average of the warped brain images. Proximity to white matter tracts was determined by reference to a tractographic atlas (Wakana *et al.,* 2004).

Results

Clinical and neuropathological data from the FTLD cohort are summarized in Table 1. Considering the cohort as a whole, 42 of the 95 cases (44%) had tau pathology, comprising Pick's disease ($n = 13$), pathology consistent with *MAPT* mutations ($n = 14$), corticobasal degeneration ($n = 9$) and progressive supranuclear palsy ($n = 6$); 48 (51%) had TDP-43 pathology, comprising TDP-A ($n = 25$), TDP-B ($n = 3$), TDP-C ($n = 19$) and TDP-D ($n = 1$); and five (5%) had FUS pathology, comprising atypical FTLD-U ($n = 4$) and neuronal intermediate filament inclusion disease ($n = 1$). Genetic analysis identified mutations in the *MAPT* or *GRN* genes in 22 cases (23% of the series). A pathogenic mutation was confirmed in 13 of the 14 cases with pathology consistent with a mutation in the *MAPT* gene: nine with 10 + 16 intronic mutations, two with G389R mutations and single cases with N296N and R406W mutations; DNA was not available in the remaining case. Nine of 21 TDP-A cases where DNA was available for screening had *GRN* mutations: seven with C31fs, one with Q130fs, one with 1048_1049insG. Of the remaining 12 *GRN*-mutation-negative cases with available DNA, three (25%) had the TT *GRN* 3′ untranslated region rs5848 genotype that was initially reported to be associated with FTLD-TDP (compared with 28/347 or 8% of normal controls—no significant difference, $P = 0.08$ Fisher's exact test); six cases (50%) had the CT genotype (compared with 44% of controls) and three (25%) had the CC genotype (compared with 48% of controls). Half of the cases with TDP-A pathology but without *GRN* mutations also had strong evidence of a family history: two cases had a modified Goldman score (Rohrer *et al.,* 2009) of one (autosomal dominant family history of FTLD) and four had a score of two (three or more family members with dementia). Behavioural variant FTD was the most common clinical syndrome in the series (47/95 cases, 49%), followed by semantic dementia (23/95 cases, 24%) and PNFA (10/95 cases, 11%). The five *in vivo* brain biopsy cases in this series comprised three cases of Pick's disease, one case with

Downloaded from https://academic.oup.com/brain/article/134/9/2565/419546 by guest on 23 April 2025

Table 1 Pathological and clinical summary of cases in the series

Pathology	*n* (%)	Gender, % male	Age at clinical onset, mean (SD) (years)	Age at death, mean (SD) (years)	Duration, mean (SD) (years)	Clinical presentation					
						Behavioural variant FTD	FTD/MND	Semantic dementia	PNFA	Corticobasal syndrome	PSPS
Tau	42 (44)										
Pick's disease	13 (14)	69.2	55.4 (5.8)	69.2 (3.5)[a]	12.0 (4.3)[a]	6	0	4	3	0	0
MAPT mutations	14 (15)	64.3	50.4 (8.6)	62.6 (10.4)	12.1 (4.3)	12	0	0	0	2	0
Corticobasal degeneration	9 (9)	55.6	58.2 (9.0)	67.8 (7.8)[b]	8.3 (2.2)[b]	3	0	0	4	1	1
Progressive supranuclear palsy	6 (6)	28.6	59.0 (5.2)	69.8 (36)	10.0 (1.9)	0	0	0	0	1	5
TDP-43	48 (51)										
A	25 (26) (9 *GRN*)	60.0	58.3 (6.9)	65.3 (8.2)	6.4 (2.5)	20	1	0	3	1	0
B	3 (3)	33.3	55.7 (6.7)	60.8 (5.7)	5.2 (1.0)	0	3	0	0	0	0
C	19 (20)	78.9	59.3 (6.6)	72.2 (5.9)	12.9 (2.7)	0	0	19	0	0	0
D	1 (1)	100.0	52.0	62.0	10.0	1	0	0	0	0	0
FUS	5 (5)										
Atypical FTLDU	4 (4)	100.0	45.5 (4.7)	53.9 (4.4)	8.4 (2.5)	4	0	0	0	0	0
NIFID	1 (1)	0.0	27.0	NA	NA	1	0	0	0	0	0
TOTAL	95					47	4	23	10	5	6

a Data from 10 patients.
b Data from 8 patients.
NA = not available; NIFID = neuronal intermediate filament inclusion disease; PSPS = progressive supranuclear palsy syndrome.

corticobasal degeneration and one with FUS-neuronal intermediate filament inclusion disease pathology.

Results of the quantitative analysis for coexisting pathological features of Alzheimer's disease and cerebrovascular disease are presented in Supplementary Table 1. This analysis revealed that additional pathological findings were minor in most (78/90 post-mortem) cases. No cases fulfilled Braak criteria correlating with established Alzheimer's disease based on staging of neurofibrillary tangle pathology; three cases (one in each of the corticobasal degeneration, TDP-A and TDP-C groups) additionally fulfilled Braak criteria correlating with 'mild cognitive impairment', and two of these cases also had frequent amyloid plaques and significant vascular amyloid deposition. Four other cases (one with Pick's, two with *MAPT* mutations, one with progressive supranuclear palsy pathology) showed frequent Aβ amyloid plaques based on CERAD criteria. Cerebrovascular pathology was graded as moderate in four cases (one with a *MAPT* mutation, one with corticobasal degeneration and two with FUS pathology) and severe in three cases (one in each of the progressive supranuclear palsy, TDP-A and TDP-C groups).

We now consider the histopathological associations of particular clinical syndromes and of particular atrophy patterns on volumetric MRI. We then consider the data from the complementary perspective of the histopathological substrates, considering the clinical and neuroanatomical profiles of particular pathologies.

Clinical syndromes: histopathological associations of clinical features

Histopathological associations of clinical and neuropsychological features of the cases in this series are summarized below and in the Supplementary Material.

Presentations with behavioural variant FTD were observed in association with all pathologies except TDP-C, TDP-B (associated with FTD-MND) and progressive supranuclear palsy (Supplementary Table 2). Semantic dementia was associated with TDP-C pathology in 19 of 23 cases (83%); the remaining four patients had Pick's disease (Supplementary Table 3), and the presence of acalculia (not referenced in current consensus criteria for semantic dementia: Gorno-Tempini *et al.*, 2011) appeared to be associated with underlying Pick's pathology (present in three of four patients who exhibited acalculia). PNFA was a presentation of tau pathologies in 7 of 10 cases (70%): three patients had Pick's disease, four had corticobasal degeneration (Supplementary Table 4) and orofacial apraxia developed only in patients with tau pathologies. Presentation with corticobasal syndrome was associated with tau (corticobasal degeneration, progressive supranuclear palsy or *MAPT* mutation) pathologies in four of five cases; the remaining patient had TDP-A pathology in association with a *GRN* mutation. Progressive supranuclear palsy syndrome was associated with tau pathology in all six cases; five patients had progressive supranuclear palsy pathology, while the remaining patient had corticobasal degeneration pathology. FTD-MND was associated with TDP-43 pathology in all four cases; three patients had TDP-B pathology, and the remaining patient had TDP-A pathology. Certain clinical features were observed across the cardinal syndromic groups (Supplementary Tables 2–4). Behavioural symptoms commonly developed in the course of the aphasic syndromes and in general did not discriminate between histopathological substrates. Other common features were episodic memory impairment, executive dysfunction and anomia. Visuospatial impairment and limb apraxia were not observed in association with *MAPT* mutations, TDP-C or FUS pathologies.

Downloaded from https://academic.oup.com/brain/article/134/9/2565/419546 by guest on 23 April 2025

Table 2 Volumetric imaging data for different pathological groups in FTLD cohort

	Pick's disease	*MAPT* mutations	Corticobasal degeneration	TDP-A	TDP-C	FUS-atypical FTLDU
No. of cases	9	6	5	7	12	2
Disease duration at scan, mean (SD) (years)	4.7 (1.7)	5.1 (2.4)	4.4 (0.8)	3.8 (2.0)	4.6 (2.4)	3.6 (2.9)
Total brain volume (% control mean)	88 (10)*	94 (9)	85 (6)*	86 (10)*	94 (8)*	89 (4)*
Cerebral asymmetry index[a]	4.3 (2.4)*	1.2 (0.8)*	1.3 (0.5)*	3.4 (2.7)*	3.0 (1.0)*	1.6 (0.7)*
Grey matter lobar volume (% control mean)						
Frontal	73 (14)*	92 (10)	81 (14)*	73 (11)*	95 (12)	69 (6)*
Temporal	73 (11)*	73 (7)*	87 (17)	76 (15)*	69 (11)*	81 (5)*
Parietal	88 (10)*	89 (11)*	85 (20)	82 (10)*	94 (14)	88 (11)*
Cingulate	70 (15)*	88 (18)*	82 (11)*	65 (7)*	89 (18)*	75 (16)*
Subcortical volumes (% control mean)						
Hippocampus	67 (18)*	57 (3)*	86 (16)	77 (27)*	67 (17)*	69 (3)*
Amygdala	55 (21)*	50 (11)*	80 (19)*	75 (23)*	53 (16)*	63 (3)*
Caudate	77 (12)*	87 (12)*	85 (6)*	86 (18)	89 (11)*	66 (19)*
Putamen	62 (12)*	75 (9)*	76 (11)*	75 (9)*	81 (12)*	67 (17)*
Brainstem	97 (11)	95 (10)	91 (13)	94 (11)	99 (7)	92 (19)

Only a single FUS-neuronal intermediate filament inclusion disease case was identified and so was not included in the table.
a Calculated as follows: (absolute hemispheric volume difference/whole brain volume × 100).
*Significantly different to controls, $P < 0.05$; significant volume differences between disease groups ($P < 0.05$) follow.
Total brain volume: corticobasal degeneration < TDP-C. Asymmetry index: Pick's disease > *MAPT* mutations, corticobasal degeneration, TDP-C, FUS-atypical FTLD-U; TDP-A > *MAPT* mutations, corticobasal degeneration; TDP-C > *MAPT* mutations, corticobasal degeneration, FUS-atypical FTLD-U. Frontal lobe: Pick's disease < *MAPT* mutations, TDP-C; TDP-A < *MAPT* mutations, TDP-C; FUS-atypical FTLD-U < *MAPT* mutations, TDP-C. Temporal lobe: TDP-C < corticobasal degeneration, FUS-atypical FTLD-U. Parietal lobe: TDP-A < TDP-C. Cingulate: Pick's disease < TDP-C; TDP-A < *MAPT* mutations, corticobasal degeneration, TDP-C. Hippocampus: Pick's disease < corticobasal degeneration; *MAPT* mutations < corticobasal degeneration, TDP-C; TDP-C < corticobasal degeneration. Amygdala: Pick's disease < corticobasal degeneration; *MAPT* mutations < corticobasal degeneration; TDP-C < corticobasal degeneration. Caudate: Pick's disease < TDP-C; FUS-atypical FTLD-U < TDP-C. Putamen: Pick's disease < *MAPT* mutations, corticobasal degeneration, TDP-A, TDP-C.

Volumetric magnetic resonance imaging findings: neuroimaging predictors of tissue pathology

Volumetric data for different pathological groups are presented in Table 2 and Fig. 1. The pathological groups with neuroimaging data were Pick's disease ($n = 9$), *MAPT* mutations ($n = 6$), corticobasal degeneration ($n = 5$), TDP-A ($n = 7$; four with *GRN* mutations), TDP-C ($n = 12$) and FUS pathology (two cases with atypical FTLD-U, one with neuronal intermediate filament inclusion disease). Regional volumetric data were not available for one case in the TDP-A group; the small FUS group was excluded from logistic regression analyses.

In univariate logistic regression analyses (thresholded at significance level $P < 0.05$), Pick's disease was associated with smaller mean putaminal and frontal lobe volumes, and greater hemispheric asymmetry; *MAPT* mutations with less hemispheric asymmetry; corticobasal degeneration with larger mean hippocampal, amygdala and temporal lobe volumes and with less hemispheric asymmetry (last association borderline significant, $P = 0.066$); TDP-C pathology with larger mean putaminal, cingulate and frontal lobe volumes and with smaller mean temporal lobe volume (last association borderline significant, $P = 0.069$); and TDP-A pathology with smaller cingulate volume (borderline significant, $P = 0.054$).

In multivariate analyses (all thresholded at significance level $P < 0.05$), Pick's disease was associated with the combination of smaller putaminal volume with greater hemispheric asymmetry; *MAPT* mutations with less hemispheric asymmetry; corticobasal degeneration with the combination of larger hippocampal volume with less hemispheric asymmetry; and TDP-C with the combination of smaller temporal lobe volume with larger frontal lobe volume.

Histopathological substrates: clinical profiles of tissue pathology

Pick's disease

In the 13 patients with Pick's disease, the initial clinical syndrome was behavioural variant FTD in six cases, PNFA in three cases and semantic dementia in four cases. Cases with semantic dementia on the basis of Pick's disease were more likely to have acalculia than cases with semantic dementia with TDP-C pathology (Supplementary Table 3). Asymmetric limb apraxia (more severe contralateral to the maximally atrophic hemisphere) in keeping with corticobasal syndrome developed subsequently in two patients presenting with behavioural variant FTD and one presenting with PNFA. Parkinsonism developed in two patients. Unexplained episodes of sudden collapse with loss of consciousness developed in two patients, and one patient reported an alteration of visual perception (washes of red over the visual scene without formed visual hallucinations). Certain features became prominent later in the disease course for the Pick's disease group as a whole: progressive reduction in spontaneous speech leading to mutism

Downloaded from https://academic.oup.com/brain/article/134/9/2565/419546 by guest on 23 April 2025

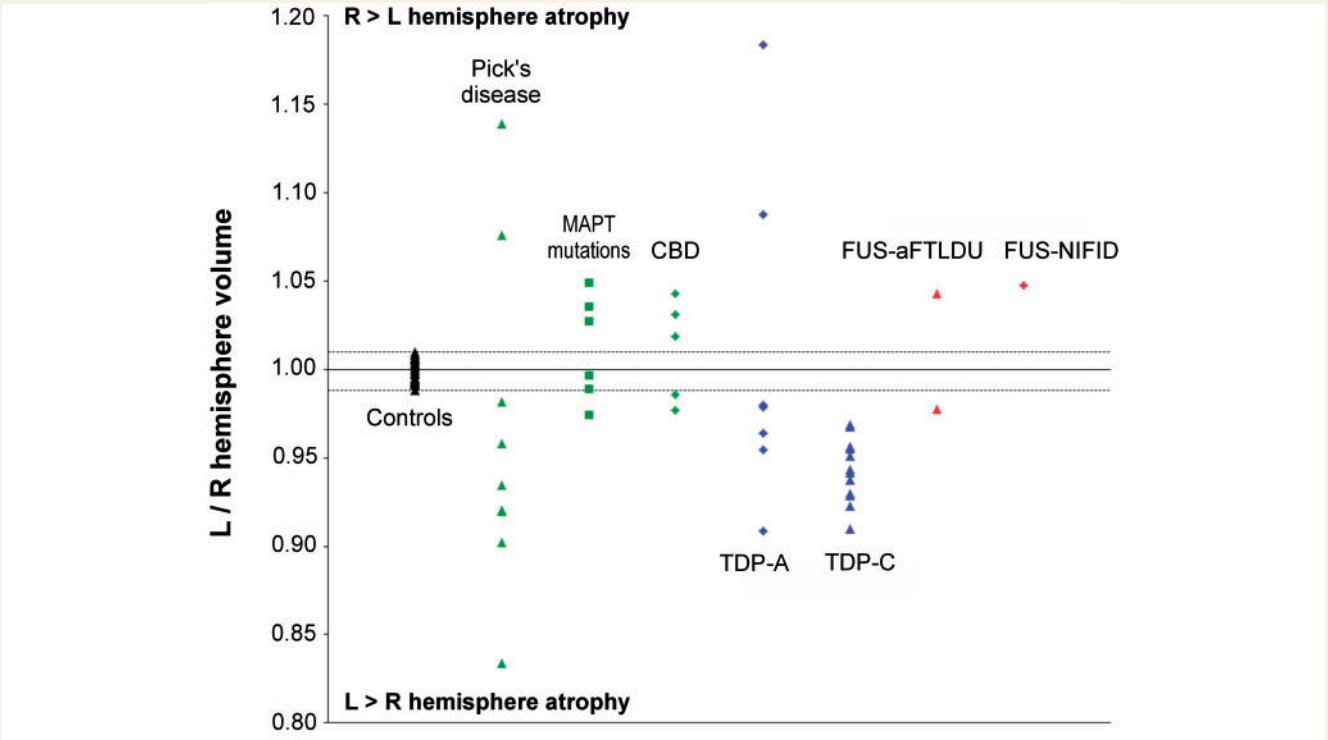

Figure 1 Cerebral interhemispheric asymmetry in FTLD pathological groups and in healthy controls. For display purposes, hemispheric asymmetry is here expressed as the ratio of left/right hemisphere volumes for each subject. Horizontal lines indicate healthy control range aFTLDU = atypical FTLDU; CBD = corticobasal degeneration; NIFID = neuronal intermediate filament inclusion disease.

occurred in all patients irrespective of the presenting syndrome and impaired single word comprehension developed in the majority.

MAPT mutations

Twelve of the 14 patients in the *MAPT* mutation group presented with behavioural variant FTD; the remaining cases presented with corticobasal syndrome. These cases have been previously reported (Rohrer *et al.*, 2009). All patients (including the nine cases with 10 + 16 intronic mutations) presenting with behavioural variant FTD syndrome had prominent disinhibition and developed semantic impairment with profound anomia and episodic memory impairment as the disease progressed. Parkinsonism developed in five cases.

Corticobasal degeneration

In the nine patients with corticobasal degeneration pathology, the initial clinical syndrome was variable: three patients had behavioural variant FTD, four had PNFA, one had corticobasal syndrome and one had progressive supranuclear palsy syndrome. However, corticobasal syndrome developed later in the course in four patients presenting with an alternative clinical syndrome (one behavioural variant FTD, two PNFA and one progressive supranuclear palsy syndrome). Most patients exhibited behavioural abnormalities and all developed word-finding difficulty over the course of the illness. Parkinsonism was seen in five cases.

Progressive supranuclear palsy

Progressive supranuclear palsy pathology was associated with progressive supranuclear palsy syndrome in all but one case who had corticobasal syndrome.

TDP-A pathology

Twenty of the 25 patients with TDP-A pathology presented with behavioural variant FTD. Of the remaining patients, three presented with PNFA, one with corticobasal syndrome and one with FTD/MND. Excluding patients for whom no DNA was available, we compared the TDP-A subgroup with *GRN* mutations (nine patients) with the subgroup lacking *GRN* mutations (12 patients); results are summarized in Supplementary Table 5. Considering the neuropsychological profiles early in the course, executive dysfunction was present in all patients assessed and episodic memory impairment was frequent in both subgroups, while parietal lobe dysfunction (characterized by limb apraxia, dyscalculia or visuospatial impairment) was also common, though somewhat more frequent in the *GRN* mutation subgroup. The *GRN*-mutation-negative patient with progressive aphasia presented with reduced speech output and anomia without speech apraxia but with emergence of a single word comprehension deficit, consistent with previous descriptions of *GRN*-related progressive aphasia (Rohrer *et al.*, 2010*a*). A similar range of behavioural symptoms was seen in the subgroups with and without *GRN* mutations: apathy was the most frequent behavioural abnormality in both

Downloaded from https://academic.oup.com/brain/article/134/9/2565/419546 by guest on 23 April 2025

subgroups, while hallucinations and delusions were also exhibited by patients in each subgroup.

TDP-B pathology

All patients in this group had FTD-MND presenting as a behavioural syndrome with features of MND supervening later in the course. All patients exhibited disinhibition, apathy, loss of empathy, perseverative or obsessional behaviours and appetite changes, and one patient had prominent delusions (Omar *et al.*, 2009). This group had the shortest mean clinical disease duration [5.2 (SD 1.0) years] of the entire FTLD cohort.

TDP-C pathology

All patients in this group presented with semantic dementia. This group had the longest mean clinical disease duration [12.9 (SD 2.7) years] of the entire FTLD cohort.

TDP-D pathology

A single patient was found to have TDP-D pathology although DNA was not available for genetic analysis. He developed progressive muscle weakness (diagnosed as 'spinal muscular atrophy') at the age of 49 years, followed 3 years later by progressive behavioural and cognitive impairment. His brother also had a diagnosis of 'spinal muscular atrophy' with onset in his 50s, his sister had been diagnosed with dementia in her 50s and his mother had died of 'dementia' aged 55 years. Neuropsychological assessment six years after the onset of cognitive impairment revealed anomia, dyslexia, dysgraphia and dyscalculia with relatively intact episodic memory and right hemisphere functions. Neurological examination at this time revealed bilateral facial weakness and proximal limb weakness. Brain CT revealed asymmetrical atrophy maximally affecting the left cerebral hemisphere.

FUS pathology

All patients with FUS pathology presented with behavioural variant FTD. The single patient with neuronal intermediate filament inclusion disease had dysarthria and limb apraxia, while the four patients with atypical FTLD-U had a normal neurological examination. This group had the earliest clinical onset of the entire FTLD cohort [atypical FTLD-U, mean age at onset 45.5 (SD 4.7) years; neuronal intermediate filament inclusion disease, age at onset 27 years]. These five patients have been described previously (Rohrer *et al.*, 2010*c*).

Histopathological substrates: neuroanatomical profiles of tissue pathology

Volumetric magnetic resonance imaging profiles

Particular tissue pathologies were associated with distinctive profiles of regional brain atrophy relative to healthy controls (summarized in Table 2). Pick's disease was associated with asymmetric, predominantly frontal and temporal lobe atrophy with additional severe involvement of cingulate and putamen. *MAPT* mutations were associated with largely symmetric, predominantly temporal lobe atrophy. Corticobasal degeneration was associated with symmetric, rather diffuse atrophy, accentuated in the frontal lobes but with wide individual variation. TDP-C was associated with asymmetric atrophy predominantly involving the temporal lobes. TDP-A was associated with asymmetric atrophy with a frontal emphasis but extending rather diffusely within the more affected hemisphere to involve the parietal lobe and with marked involvement of the cingulate. Within the TDP-A group, the most asymmetric interhemispheric atrophy was associated with *GRN* mutations. FUS-atypical FTLD-U (based on only two cases with MRI) was associated with largely symmetric atrophy, most marked in the frontal lobes but also involving the temporal lobes and with severe involvement of caudate.

An important issue in FTLD concerns the extent to which neuroimaging features reflect clinical syndromes versus underlying tissue pathologies. We therefore also consider the volumetric profiles associated with tissue pathologies within each of the major syndromic groups (Supplementary Tables 2–4). Comparing within-syndrome subgroup-level profiles for pathologies represented in more than one syndromic group (Pick's, TDP-A and corticobasal degeneration), Pick's disease (irrespective of the clinical syndrome) was consistently associated with asymmetric, predominantly frontotemporal, cingulate and putaminal atrophy and TDP-A with asymmetric frontoparietal and cingulate atrophy, while corticobasal degeneration was associated with more symmetric and more diffuse atrophy. However, there was also evidence that clinical syndrome modulates the regional distribution of atrophy: in the Pick's disease subgroup, temporal lobe atrophy was more marked for cases presenting with semantic dementia than with other clinical syndromes. Conversely, within the semantic dementia syndromic group, the Pick's and the TDP-C pathological groups exhibited very similar profiles of atrophy within the temporal lobe but the Pick's disease subgroup was associated with more marked asymmetry of temporal lobe involvement and additionally associated with more marked, asymmetric parietal lobe atrophy (Supplementary Table 3).

Significant neuroanatomical volumetric differences between pathological groups

Disease-associated neuroanatomical profiles were substantiated by direct statistical comparisons of volumetric data between the pathological groups (all $P < 0.05$). Total brain volume was significantly smaller in the corticobasal degeneration group than the TDP-C group. Interhemispheric cerebral asymmetry was significantly greater in the Pick's disease, TDP-A and TDP-C groups than the *MAPT* mutation, corticobasal degeneration and FUS-atypical FTLD-U groups. Frontal lobe volume was significantly smaller in the Pick's disease, TDP-A and FUS-atypical FTLD-U groups than the *MAPT* mutation and TDP-C groups. Temporal lobe volume was significantly smaller in the TDP-C group than the corticobasal degeneration and FUS-atypical FTLD-U groups; while hippocampal and amygdala volume was significantly smaller in the Pick's, *MAPT* mutation and TDP-C groups than in the corticobasal degeneration group. Parietal lobe volume was significantly smaller in the TDP-A group than the TDP-C group. Cingulate volume was significantly smaller in the Pick's group than the TDP-C group, and significantly smaller in the TDP-A group than the *MAPT* mutation, corticobasal degeneration and TDP-C groups. Caudate volume

Downloaded from https://academic.oup.com/brain/article/134/9/2565/419546 by guest on 23 April 2025

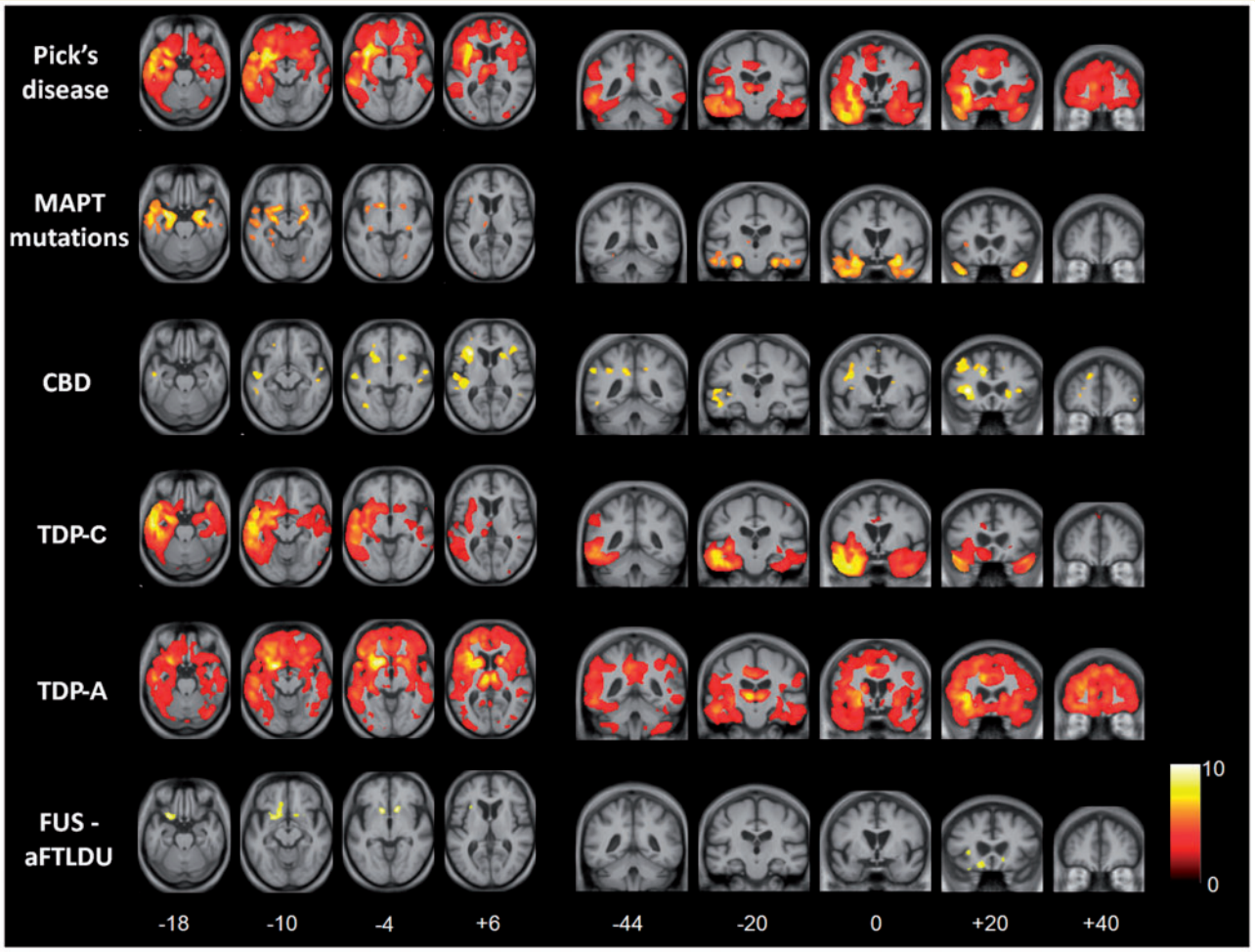

Figure 2 Voxel-based morphometry analysis on grey matter regions in FTLD pathological groups relative to healthy controls. Statistical parametric maps have been thresholded at $P < 0.01$ after false discovery rate correction over the whole-brain volume and rendered on axial (*left*) and coronal (*right*) sections of a study-specific average group T_1-weighted MRI template image in DARTEL space. The colour bar (*lower right*) indicates the *t*-score. This analysis was performed on flipped images (see text). For ease of comparison, the same brain template sections are shown for each pathological group; co-ordinates (mm) for the plane of each section are indicated below. aFTLDU = atypical FTLDU; CBD = corticobasal degeneration.

was significantly smaller in the Pick's and FUS-atypical FTLD-U groups than the TDP-C group. Putaminal volume was significantly smaller in the Pick's group than the *MAPT* mutation, corticobasal degeneration, TDP-A and TDP-C groups.

In summary, these data provide quantitative support for distinctive neuroanatomical profiles of pathologies in the FTLD spectrum. Pick's, TDP-A and TDP-C were associated with more marked interhemispheric asymmetry than other pathological groups. Within an affected hemisphere, TDP-C pathology and *MAPT* mutations were associated with relatively focal temporal lobe atrophy, while other pathologies were associated with more widespread cortical atrophy and variable involvement of subcortical nuclei.

Voxel-based morphometry profiles

The voxel-based morphometry analysis of regional atrophy in each of the pathological groups corroborated the results of MRI volumetry. Representative sections showing profiles of tissue loss are displayed in Figs 2 and 3, and brain regions involved are summarized in Table 3; these analyses are based on flipped images (following the procedure described in the 'Materials and methods' section), in order to capture directional asymmetries that might be evident only at individual subject level. All results are reported with reference to the healthy control group; direct comparisons between disease groups did not yield significant grey matter associations at the prescribed significance threshold.

Relative to healthy controls, the patient groups with *MAPT* mutations, with TDP-C pathology and with FUS pathology had relatively localized profiles of grey and white matter loss. In the *MAPT* mutation group, grey matter loss was relatively symmetric between the cerebral hemispheres and most marked in medial and anterior inferior temporal cortex with less marked involvement of orbitofrontal cortex and insula; localized white matter loss was

Downloaded from https://academic.oup.com/brain/article/134/9/2565/419546 by guest on 23 April 2025

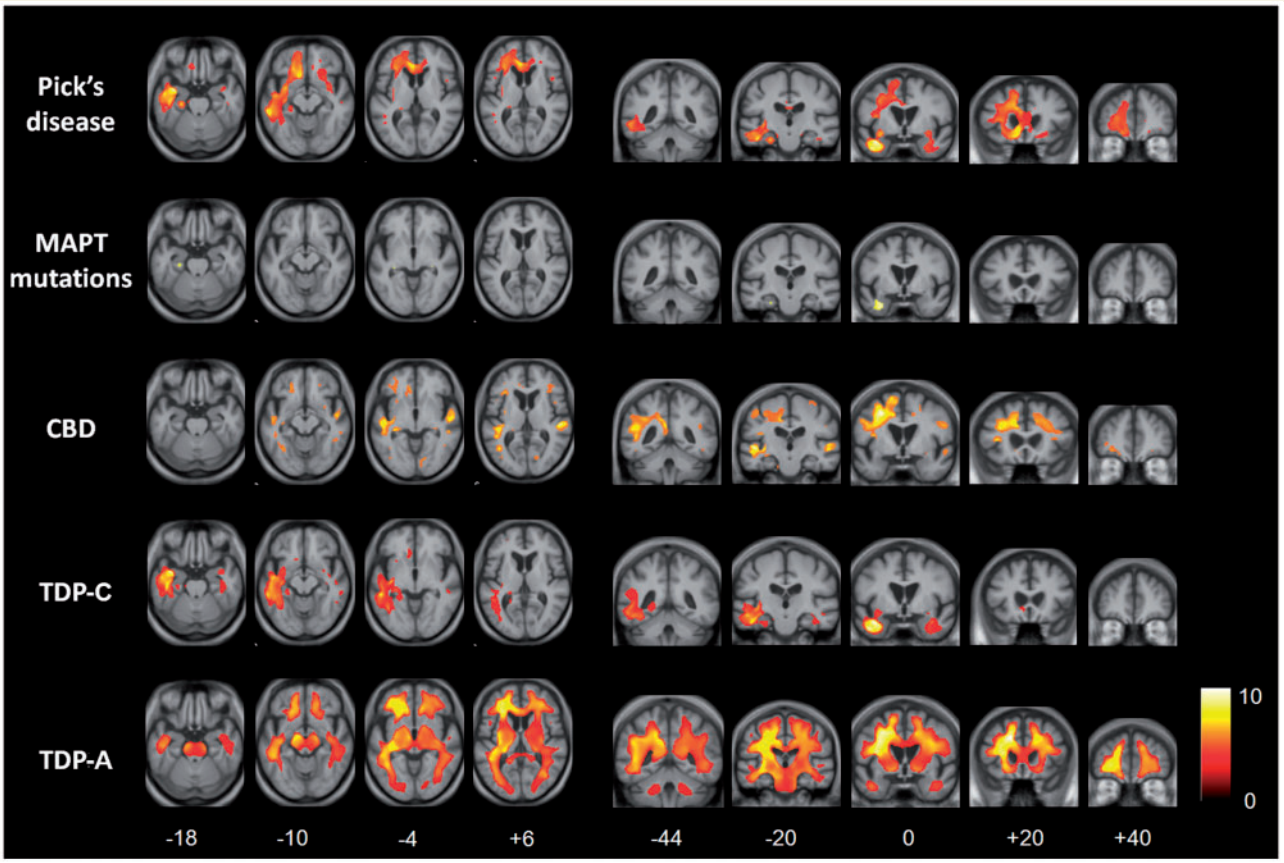

Figure 3 Voxel-based morphometry analysis on white matter regions in FTLD pathological groups relative to healthy controls. Statistical parametric maps have been thresholded at $P < 0.01$ after false discovery rate correction over the whole-brain volume and rendered on axial (*left*) and coronal (*right*) sections of a study-specific average group T_1-weighted MRI template image in DARTEL space. The colour bar (*lower right*) indicates the *t*-score. This analysis was performed on flipped images (see text). For ease of comparison, the same brain template sections are shown for each pathological group; co-ordinates (mm) for the plane of each section are indicated below.
CBD = corticobasal degeneration.

Table 3 Grey and white matter regions predominantly involved in voxel-based morphometry analysis of FTLD pathologies

	Grey matter												White matter					
	Frontal			Temporal					Parietal		Subcortical							
	dFL	ACC	OFC	sTL/Ins	TP	mTL	iTL	pTL	PCC/PC	LPL	BG	Thal	SLF	ILF	UF	CC	Fornix	Brainstem
Pick's disease	+	+	+	+	+	+	+	+	+	+	+	+	+	+	+	+	+	
MAPT mutations			+	+	+	+	+							+			+	
Corticobasal degeneration	+	+		+				+	+	+	+		+	+				
TDP-A	+	+	+	+	+	+	+	+	+	+	+	+	+	+		+		+
TDP-C		+	+	+	+	+	+	+						+	+		+	
FUS			+	+							+							

Involved regions (coded +) are based on the contrast between the disease group and healthy control subjects, at a voxel-wise significance threshold $P < 0.01$ corrected over the whole brain volume.
ACC = anterior cingulate cortex; BG = basal ganglia; CC = corpus callosum; dFL = dorsolateral frontal lobe; ILF = inferior longitudinal fasciculus; iTL = inferior temporal lobe; Ins = insula; LPL = lateral parietal lobe; MAPT = microtubule-associated protein tau; mTL = medial temporal lobe; OFC = orbitofrontal cortex; PC = precuneus; PCC = posterior cingulate cortex; pTL = posterior temporal lobe; SLF = superior longitudinal fasciculus; sTL = superior temporal lobe; TDP-A = TAR-DNA-binding protein-43 type A pathology; TDP-C = TAR-DNA-binding protein-43 type C pathology; Thal = thalamus; TP = temporal pole; UF = uncinate fasciculus.

evident in the region of the anterior inferior longitudinal fasciculus and fornix. In the TDP-C group, there was asymmetric grey matter loss predominantly involving the temporal poles and anterior inferior temporal cortex with less marked involvement of orbitofrontal cortex, insula and anterior cingulate; white matter loss was evident predominantly in the region of the inferior longitudinal fasciculus, uncinate fasciculus and fornix. In the FUS group, there was relatively symmetric grey matter loss

Downloaded from https://academic.oup.com/brain/article/134/9/2565/419546 by guest on 23 April 2025

predominantly involving orbitofrontal cortex, insula and caudate nuclei; there was no significant white matter involvement.

More extensive profiles of tissue loss were evident in the patient groups with Pick's disease, corticobasal degeneration and TDP-A pathology. In the Pick's disease group, there was asymmetric grey matter loss predominantly involving dorsolateral and orbitofrontal cortex, insula, anterior temporal lobe, anterior cingulate, putamen and thalamus, with less marked involvement of more posterior temporal cortex, precuneus and anterior parietal cortex and caudate; white matter loss predominantly occurred in the region of the anterior inferior longitudinal fasciculus, superior longitudinal fasciculus and corpus callosum. In the corticobasal degeneration group, grey matter loss was relatively symmetric and most marked in the dorsolateral frontal cortex, insula, superior temporal cortex, anterior cingulate and caudate, with less marked involvement of precuneus and inferior parietal cortex; white matter loss was most marked in the region of the superior longitudinal fasciculus and inferior longitudinal fasciculus. In the TDP-A group, there was asymmetric but extensive grey matter loss most markedly involving dorsolateral and orbitofrontal cortex, insula, anterior, middle and inferior temporal cortex, anterior cingulate, thalamus and caudate, with less marked involvement of precuneus and inferior parietal cortex; there was associated extensive white matter loss in the region of the superior longitudinal fasciculus, inferior longitudinal fasciculus, corpus callosum and fibre projection pathways via the brainstem.

Post hoc cluster analysis

Whereas voxel-based morphometry can identify group-level disease signatures, it does not assess individual variation in neuroanatomical profiles within disease groups. Here we used a *post hoc* hierarchical cluster analysis (Everitt *et al.,* 2001; further details in Supplementary Material) to further investigate the hypothesis that the individuals comprising the FTLD cohort could be partitioned using neuroanatomical profiles according to pathological diagnosis. Motivated by the results of the voxel-based morphometry analysis, for each subject we derived three measures based on lobar grey matter volumes: a measure of the extent of frontal lobe (extratemporal) versus temporal lobe involvement (the difference between mean frontal and temporal lobe grey matter volumes, each normalized to the corresponding control mean lobar grey matter volume); a measure of inter temporal asymmetry (the modulus of the difference between right and left temporal lobe grey matter volumes, normalized to the control mean temporal lobe grey matter volume); and a measure of inter-frontal asymmetry (the modulus of the difference between right and left frontal lobe grey matter volumes, normalized to the control mean frontal lobe grey matter volume).

Cluster analyses based on each of these measures partitioned the FTLD cohort into two subgroups (Fig. 4; details provided in Supplementary Material); taken together, these analyses partitioned the FTLD cohort into at least four pathological subgroups (Pick's, *MAPT*, TDP-C, corticobasal degeneration/FUS), in alignment with the group-level voxel-based morphometry findings (Fig. 5). TDP-C pathology was consistently associated with focal, asymmetric temporal lobe atrophy; *MAPT* mutations with focal relatively symmetric temporal lobe atrophy; Pick's disease with asymmetric extra temporal atrophy; and corticobasal degeneration and FUS pathology with relatively symmetric, extra temporal atrophy. Pick's disease cases showed the most variation in regional atrophy profile, a substantial proportion of cases showing asymmetric temporal in addition to frontal lobe atrophy. There was also substantial individual variation within the TDP-A group: the majority of cases showed extratemporal atrophy; however, the degree of asymmetry varied widely between individuals in this group.

It is noteworthy that the difference measures were less useful for differentiating cases on clinical syndromic rather than pathological grounds: the inter temporal asymmetry measure separated cases with semantic dementia from other syndromic groups (consistent with the close association between semantic dementia and TDP-C pathology), but the neuroimaging metrics used here did not resolve the PNFA and behavioural variant FTD syndromic groups (Fig. 4).

Discussion

Here we have presented clinical and neuroanatomical findings in a large series of patients representing the major pathologies of the FTLD spectrum. The findings underline the clinical, anatomical and pathological heterogeneity of these diseases and corroborate the evidence of previous pathological series (Hodges *et al.,* 2004; Kertesz *et al.,* 2005; Forman *et al.,* 2006; Josephs *et al.,* 2006*a*, *b*, 2008*b*, 2009; Snowden *et al.,* 2007; Geser *et al.,* 2009; Whitwell *et al*., 2009*b*, *d*; Rohrer *et al.,* 2010*b*). Convergent neuroanatomical data from volumetric, voxel-based morphometry and cluster analyses suggest a framework for classifying FTLD pathologies according to their neuroanatomical atrophy profiles across the brain: rather than regional anatomical or syndromic associations, this framework (Fig. 5) is based on pathologically determined network disintegration.

Clinical associations of frontotemporal lobar degeneration pathologies

Considering the series firstly from a clinical perspective, certain relatively specific clinicopathological associations were confirmed: semantic dementia with TDP-C pathology; FTD-MND with TDP-B pathology; young-onset behavioural variant FTD with FUS pathology; and progressive supranuclear palsy syndrome with progressive supranuclear palsy pathology. PNFA was most commonly associated with tau pathologies, also in line with previous evidence (Josephs *et al.,* 2006*a*); this association may be more specific for PNFA accompanied by speech apraxia, consistent with present evidence that orofacial apraxia accompanies tau but not TDP pathology. However, behavioural variant FTD (the most common clinical syndrome across the present FTLD cohort) was histopathologically heterogeneous. Similar diversity was evident when considering the clinical associations of particular pathological entities. Pick's disease was clinically heterogeneous: though 3R-tau-defined Pick's disease has been relatively little studied, this heterogeneity is in line with previously reported

Downloaded from https://academic.oup.com/brain/article/134/9/2565/419546 by guest on 23 April 2025

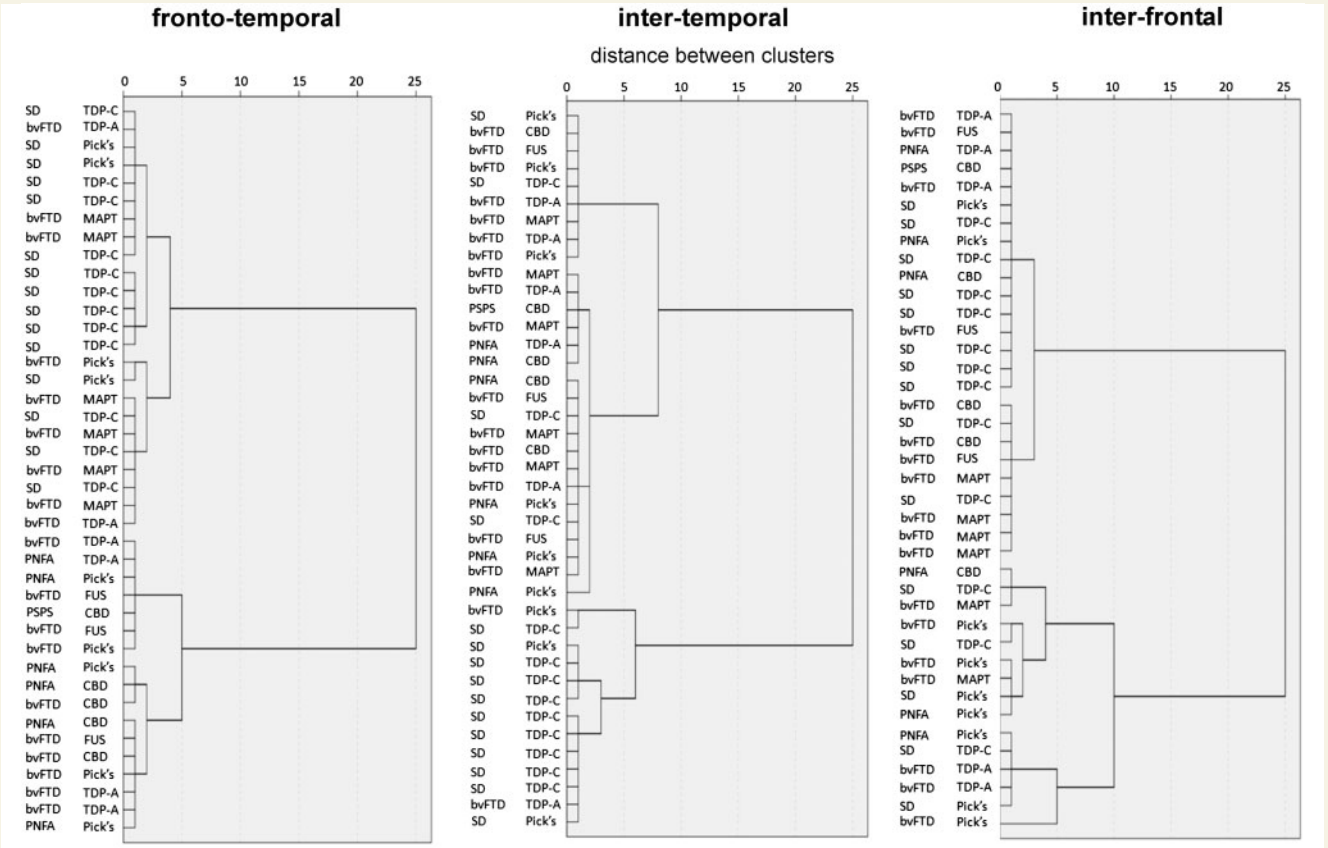

Figure 4 Cluster analyses of the FTLD cohort. Cluster analyses are shown for pathological (right-hand text column for each panel) and clinical syndromic diagnoses, according to frontotemporal, intertemporal and interfrontal volumetric difference measures (see text). Cluster dendrograms use average linkage between groups. Each cluster dendrogram demonstrates separation of the entire FTLD group into two subgroups based on the corresponding difference measure; together, the measures partition the cohort into at least four pathological subgroups (Pick's, MAPT, TDP-C, corticobasal degeneration/FUS; Fig. 5). bvFTD = behavioural variant FTD; CBD = corticobasal degeneration; PSPS = progressive supranuclear palsy syndrome; SD = semantic dementia.

clinicopathological series (Hodges *et al.*, 2004; Kertesz *et al.*, 2005; Shi *et al.*, 2005; Forman *et al.*, 2006; Josephs *et al.*, 2006*b*; Lladó *et al.*, 2008; Mesulam *et al.*, 2008; Yokota *et al.*, 2009; summarized in Supplementary Table 6). Our series reaffirms the clinical heterogeneity of corticobasal degeneration (Tang-Wai *et al.*, 2003; Murray *et al.*, 2007; Josephs and Duffy, 2008*a*; Vanvoorst *et al.*, 2008; Ling *et al.*, 2010). The clinical features of TDP-A pathology in our series were similar whether or not associated with a *GRN* mutation (see Supplementary Table 5).

Neuroanatomical associations of frontotemporal lobar degeneration pathologies

No single cortical or subcortical region was specifically involved in association with a particular pathological process. However, pathological groups varied substantially in the hemispheric distribution of atrophy. This variation was evident at group level, in a quantitative volumetric analysis of preselected brain regions (Table 2) and in a qualitative but unbiased comparison of atrophy profiles (using voxel-based morphometry, Table 3); and after taking individual variation into account, in a cluster analysis (Fig. 4). In particular, the pathological groups here segregated according to whether they were associated with relatively symmetric versus strongly asymmetric involvement of the cerebral hemispheres (Table 2, Figs 1 and 4), and whether they were associated with relatively localized temporal versus extra temporal atrophy within an affected hemisphere (Table 3, Figs 2–4).

Considering firstly the relative degree of cerebral asymmetry (the more directly quantifiable factor), *MAPT* mutations, corticobasal degeneration and FUS pathology were each associated at group level with relatively symmetric hemispheric atrophy; whereas Pick's disease, TDP-A and TDP-C pathology were each associated at group level with strongly asymmetric hemispheric atrophy. In addition to the extent of cerebral asymmetry, FTLD pathologies here could be grouped according to the extent of intra-hemispheric atrophy. *MAPT* mutations and TDP-C pathology each produced a relatively localized profile of atrophy maximally affecting the temporal lobes. *MAPT* mutations were associated with anteromesial temporal lobe atrophy; while there is a need for caution in attributing a common voxel-based morphometry profile to *MAPT* mutations considered as a group (Whitwell *et al.*, 2009*a*), case numbers here as in previous single-centre

Downloaded from https://academic.oup.com/brain/article/134/9/2565/419546 by guest on 23 April 2025

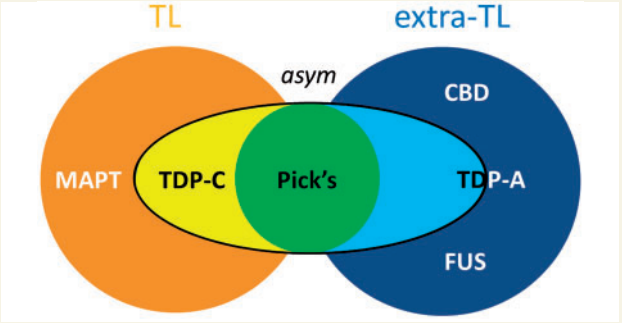

Figure 5 Diagrammatic summary of neuroanatomical features associated with pathological diagnosis in this FTLD cohort. The figure is based on volumetric, voxel-based morphometry and cluster analyses of the present neuroimaging data. Diseases can in general be classified according to whether they produced relatively focal temporal lobe atrophy (TL) or atrophy predominantly involving extratemporal (extra-TL; e.g. frontal lobe) regions; and according to whether they produced relatively symmetric or strongly asymmetric atrophy. Pick's disease was associated with an asymmetric atrophy profile variably involving temporal or extra temporal regions. TDP-A was associated with strongly asymmetric atrophy (especially in association with GRN mutations) but with wide individual variability.
CBD = corticobasal degeneration.

series were too small to attempt any more detailed mutation-specific analysis. These findings are consistent with previous neuroanatomical evidence from other series (Josephs *et al*., 2009; Pereira *et al.,* 2009; Whitwell *et al.,* 2009*a*, *b*). In contrast, Pick's disease, TDP-A and corticobasal degeneration pathology each produced widespread atrophy of cortical and subcortical regions and their connections. The atrophy profiles in these diseases overlapped extensively in frontal, temporal, parietal and subcortical areas within an affected hemisphere. These findings are in keeping with other neuroanatomical evidence for pathologically defined Pick's disease (Whitwell *et al*., 2009*b*, 2011), TDP-A pathology (Rohrer *et al.,* 2010*b*; Whitwell *et al*., 2011) and corticobasal degeneration (Josephs *et al.,* 2008*b*, 2010; Whitwell *et al*., 2011). The wide variation in individual profiles within the TDP-A group (Figs 1 and 4) suggests that other factors (for example, the presence of a *GRN* mutation) may modulate the macro-anatomical expression of TDP-A. Corticobasal degeneration is often considered an asymmetric disease on clinical and neuropsychological grounds; however, quantitative studies of atrophy in pathologically proven corticobasal degeneration have not demonstrated striking hemispheric asymmetry; a previous voxel-based morphometry study (Josephs *et al.,* 2008*b*) demonstrated distributed frontoparietal cortical, insula, posterior temporal and caudate involvement similar to the present findings. FUS pathology here involved predominantly extratemporal fronto-subcortical circuitry (including, in particular, the caudate nuclei) but with a relatively localized and symmetrical distribution; this is consistent with limited previous evidence (Josephs *et al.,* 2010).

Considering these neuroanatomical data together, we propose that FTLD-associated pathologies can be segregated based on their cerebral atrophy profiles, according to the following scheme: asymmetric, relatively localized (predominantly temporal lobe) atrophy (TDP-C); relatively symmetric, relatively localized (predominantly temporal lobe) atrophy (*MAPT* mutations); strongly asymmetric, distributed atrophy (Pick's, TDP-A); and relatively symmetric, predominantly extratemporal atrophy, which may be either distributed (corticobasal degeneration) or relatively localized (FUS).

Network signatures of frontotemporal lobar degeneration pathology: a clinico-anatomical formulation

If indeed tissue pathologies within the FTLD spectrum have separable neuroanatomical signatures, how can this be reconciled with the extensive clinical and anatomical overlap among these diseases, which was evident here as in most previous series (Pereira *et al.,* 2009; Weintraub and Mesulam, 2009; Whitwell *et al.,* 2009*b*, *c*)? There are at least two complementary clinico-anatomical formulations that might potentially reconcile clinical heterogeneity with relative anatomical specificity. First, the canonical FTLD clinical syndromes of behavioural variant FTD and PNFA both involve multi-component cognitive functions: clinical similarities might therefore arise from quite distinct pathophysiological and neuroanatomical mechanisms; and indeed, the syndromes of behavioural variant FTD and PNFA in this series were associated with substantial clinical and anatomical heterogeneity (Supplementary Tables 2 and 4), supporting previous formulations (Josephs *et al.,* 2006*a*, 2009; Whitwell *et al.,* 2009*b*). Secondly, the pathological processes associated with these syndromes tend to involve distributed hemispheric areas and their connections. A disease process beginning in one region of the hemisphere might produce a clinical syndrome distinct from that produced by the same disease process beginning in another, remote cerebral region; initial involvement of the right frontal lobe (irrespective of the pathological process) may be more likely to present as behavioural variant FTD, initial involvement of left frontal cortex as PNFA and initial involvement of more posterior cortices as corticobasal syndrome. If, however, pathological processes evolve in an anatomically restricted manner, then convergence of clinical syndromes should occur in a predictable sequence over time. Such a clinico-anatomical convergence would be consistent with previous evidence (in, for example, corticobasal degeneration and Pick's disease: Kertesz *et al.,* 2005; Sanchez-Valle *et al.,* 2006; Geda *et al.,* 2007; Yokota *et al.,* 2009; Rogalski *et al.,* 2011) and also with the present data. This interpretation allows for fine-grained clinical and anatomical differentiation within a broad syndrome category, according to the underlying pathological process (Supplementary Tables 2–4); for example, the present findings suggest that semantic dementia variants may be clinically and anatomically differentiable.

The synthesis we present here is compatible with previous evidence for differentiable neuroanatomical associations of FTLD pathologies (Josephs *et al.,* 2009; Whitwell *et al.,* 2009*a*, *b*, 2011; Rohrer *et al.,* 2010*b*). Here, we extend this synthesis across the breadth of the FTLD spectrum, taking into account

Downloaded from https://academic.oup.com/brain/article/134/9/2565/419546 by guest on 23 April 2025

the current neuropathological differentiation of these diseases rather than broad groupings such as FTLD-tau or FTLD-TDP. We do not claim that particular FTLD pathologies show specificity for a particular brain region: rather, we argue that specificity emerges as a profile of involvement across multiple anatomical regions. It is increasingly recognized that neurodegenerative diseases target large-scale neural networks that have an intrinsic connectivity laid down in the healthy brain (Seeley *et al.,* 2009). It is known that Alzheimer's disease and non-Alzheimer pathologies target distinct cerebral networks (Zhou *et al.,* 2010); however, most previous correlative studies of network breakdown in FTLD have focused on syndromes rather than histopathological substrates. Thus, the behavioural variant FTD syndrome implicates an anterior fronto-subcortical network that mediates goal-directed social behaviours (Seeley *et al.,* 2007). In contrast, the syndromes of PNFA and semantic dementia implicate dominant hemispheric dorsal fronto-insulo-parietal and anterior temporo-ventrofrontal networks mediating aspects of language output and comprehension, respectively (Saur *et al.,* 2008; Seeley *et al.,* 2009). Each of these networks was implicated (to a variable degree) by the spectrum of FTLD pathologies in the present series (Figs 2 and 3, Table 3): the anterior fronto-subcortical network particularly with Pick's, corticobasal degeneration, TDP-A and FUS pathology; the dorsal fronto-insulo-parietal network with Pick's, corticobasal degeneration and TDP-A pathology; and the anterior temporo-ventrofrontal network with TDP-C, Pick's, MAPT and TDP-A pathology. However, the neuroanatomical framework we propose here primarily addresses pathology rather than clinical syndrome; we argue that any account of neural network degeneration must ultimately take the underlying pathological substrate into account. Since clinical syndromes are associated with involvement of particular brain networks (Seeley *et al.,* 2009) and since particular pathologies often produce more than one clinical syndrome (Table 1, Supplementary Tables 2–4), in general the effects of a particular pathological substrate will be expressed in more than one functional network (though there may be important exceptions; for example, the effects of TDP-C may be largely restricted to a single anterior temporo-ventrofrontal network).

We propose that pathologies in the FTLD spectrum target distributed brain networks in a predictable manner. Specifically, we propose that the pattern of network disintegration in these diseases is determined by the interaction of at least two key factors: the distribution of the disease interhemispherically, and the distribution of the disease within a hemisphere. These factors could, in principle, operate over any individual brain region or brain network; together, however, they tend to constrain the macro-anatomical profile of the disease. According to this formulation, the neuroanatomical specificity of these diseases is likely primarily to reflect underlying network morphology (the characteristics of the fibre tracts and synaptic connections that compose the network, and allow disease spread). The local mechanisms that translate molecular lesions to neural network dysfunction remain largely unknown; however, candidate mechanisms are likely to include loss of regulatory or trophic factor support acting on synapses or glial structures, propagation of toxic molecules and disturbed network homeostasis (Seeley, 2008, 2009). The microscopic organization of a neural network could confer relative vulnerability or resistance to such mechanisms; the macroscopic expression of the pathological process would then depend on interaction of the causative lesion with critical network elements. For example, the large projection neurons of Von Economo that mediate focal network disintegration underpinning behavioural variant FTD are vulnerable to both tau and TDP-43 pathology but apparently resistant to Alzheimer pathology (Seeley, 2008), while *GRN*-associated TDP-43 inclusions have been shown to target the dominant hemispheric language network in a stereological analysis (Gliebus *et al*., 2010). The two-factor (cerebral asymmetry, hemispheric contiguity) classification of FTLD pathological signatures that we propose here is likely to be an oversimplification; however, certain molecular and network characteristics have been identified that could potentially interact to produce a fundamentally dichotomous partition of this kind. Examples include the dichotomy between toxic gain and loss of function among the spectrum of molecular insults causing FTLD (Winklhofer *et al.,* 2008); and the dichotomy between long-range and short-range pathways in the organization of cortical networks (Sporns and Zwi, 2004).

Future directions

This study has several important limitations that suggest directions for future work. Opportunities for anatomical and pathological correlation in less common FTLD syndromes are limited, and case numbers in this (as in previous) series were relatively small. This factor indicates a need for caution when interpreting statistical effects, limiting the power of the study to identify effects and potentially increasing susceptibility to ascertainment bias. This might in turn account for the absence or scarcity of certain FTLD phenotypes here [e.g. Alzheimer-like (Kelley *et al.,* 2009, 2010) and FTD-MND syndromes]. The study was retrospective; accordingly, neuropsychological functions could not be systematically assessed using a uniform battery. Appropriately directed and detailed neuropsychological assessment might corroborate or advance the framework suggested by neuroimaging data. Finally, the identification of a clinico-anatomical signature does not resolve the mechanism by which a particular pathological process gives rise to that signature; to define such mechanisms will require an understanding of how molecular and cellular pathophysiology acts on local neural circuitry and how local molecular processes scale up to the level of large-scale networks.

The present findings underline the need for further detailed, prospective longitudinal studies correlating tissue pathology with clinical, neuropsychological and neuroimaging features in large (ideally, multi-centre), pathologically confirmed FTLD series. Such studies should include connectivity-based methods such as diffusion tensor tractography and resting-state functional MRI that can delineate neural networks empirically (Seeley *et al*., 2009; Acosta-Cabronero *et al.,* 2011), complementing computational modelling (Fletcher and Warren, 2011) and micro-physiological (Winklhofer *et al*., 2008) approaches. Detailed regional histomorphometry will be an essential link between these levels of description (Davies *et al*., 2005; Gliebus *et al*., 2010; Piguet *et al*., 2011), by directly assessing the propensity of pathological processes to spread via local and connected neural elements and establishing

Downloaded from https://academic.oup.com/brain/article/134/9/2565/419546 by guest on 23 April 2025

the cytoarchitectural boundaries of these processes. In order to substantiate molecular specificities, anatomical associations of particular pathologies should be sought within as well as between broad syndromic categories such as behavioural variant FTD (Whitwell *et al*., 2009*b*). There is a particular need for longitudinal tracking of clinical and neuroanatomical patterns of disease evolution, to assess the extent to which syndromes transform over time and the precise sequence of such transformations. If indeed particular pathologies manifest in specific profiles of network disintegration, then longitudinal clinico-anatomical profiles are likely to be at least as informative as cross-sectional signatures (Whitwell *et al*., 2009*c*; Rogalski *et al*., 2011), and would provide a direct test of the hypotheses advanced here.

From a clinical perspective, we do not argue that the identification of group-level signatures of tissue pathology will necessarily allow accurate prediction of pathology in the individual patient. Rather, we anticipate that such signatures will suggest new network-level biomarkers and perhaps disease mechanisms. This in turn could help direct clinical trials targeting particular tissue pathologies. If distinctive clinico-anatomical signatures of FTLD pathologies can be substantiated, this would constrain the *modus operandi* governing how pathological processes are expressed in the brain: we see this as an important first step towards a molecular physiology of FTLD.

Acknowledgements

We are grateful to the MRC Neurodegenerative Diseases Brain Bank, Institute Of Psychiatry, King's College London. The Dementia Research Centre is an Alzheimer's Research UK Co-ordinating Centre. J.M.S. is a UK HEFCE Clinical Senior Lecturer. M.N.R. and N.C.F. are NIHR senior investigators.

Funding

Department of Health's NIHR Biomedical Research Centres funding scheme (to UCLH/UCL, where the work was undertaken; partial); Medical Research Council UK and the Alzheimer's Research UK (to T.R., J.H., J.M.S.); Wellcome Trust Senior Clinical Fellowship (J.D.W.).

Supplementary material

Supplementary material is available at *Brain* online.

References

Acosta-Cabronero J, Patterson K, Fryer TD, Hodges JR, Pengas G, Williams GB, et al. Atrophy, hypometabolism and white matter abnormalities in semantic dementia tell a coherent story. Brain 2011; 134 (Pt 7): 2025–35.

Alzheimer A. Uber eigenartige Krankheitsfalle des Spateren Alters. Z Ges Neurol Psychiatr 1911; 4: 356–85.

Boeve BF, Lang AE, Litvan I. Corticobasal degeneration and its relationship to progressive supranuclear palsy and frontotemporal dementia. Ann Neurol 2003; 54 (Suppl. 5): S15–9.

Braak H, Alafuzoff I, Arzberger T, Kretzschmar H, Del Tredici K. Staging of Alzheimer disease-associated neurofibrillary pathology using paraffin sections and immunocytochemistry. Acta Neuropathol 2006; 112: 389–404.

Cairns NJ, Bigio EH, Mackenzie IR, Neumann M, Lee VM, Hatanpaa KJ, et al. Consortium for Frontotemporal Lobar Degeneration. Neuropathologic diagnostic and nosologic criteria for frontotemporal lobar degeneration: consensus of the Consortium for Frontotemporal Lobar Degeneration. Acta Neuropathol 2007; 114: 5–22.

Davies RR, Hodges JR, Kril JJ, Patterson K, Halliday GM, Xuereb JH. The pathological basis of semantic dementia. Brain 2005; 128 (Pt 9): 1984–95.

de Silva R, Lashley T, Strand C, Shiarli AM, Shi J, Tian J, et al. An immunohistochemical study of cases of sporadic and inherited frontotemporal lobar degeneration using 3R- and 4R-specific tau monoclonal antibodies. Acta Neuropathol 2006; 111: 329–40.

Everitt BS, Landau S, Leese M. Cluster analysis. 4th edn. London: Hodder Arnold; 2001.

Fletcher PD, Warren JD. Semantic dementia: a specific network-opathy. J Mol Neurosci 2011. Advance Access published on June 29, 2011, doi:10.1007/s12031-011-9586-3.

Forman MS, Farmer J, Johnson JK, Clark CM, Arnold SE, Coslett HB, et al. Frontotemporal dementia: clinicopathological correlations. Ann Neurol 2006; 59: 952–62.

Geda YE, Boeve BF, Negash S, Graff-Radford NR, Knopman DS, Parisi JE, et al. Neuropsychiatric features in 36 pathologically confirmed cases of corticobasal degeneration. J Neuropsychiatry Clin Neurosci 2007; 19: 77–80.

Geser F, Martinez-Lage M, Robinson J, Uryu K, Neumann M, Brandmeir NJ, et al. Clinical and pathological continuum of multisystem TDP-43 proteinopathies. Arch Neurol 2009; 66: 180–9.

Gliebus G, Bigio EH, Gasho K, Mishra M, Caplan D, Mesulam MM, et al. Asymmetric TDP-43 distribution in primary progressive aphasia with progranulin mutation. Neurology 2010; 74: 1607–10.

Gorno-Tempini ML, Hillis AE, Weintraub S, Kertesz A, Mendez M, Cappa SF, et al. Classification of primary progressive aphasia and its variants. Neurology 2011; 76: 1006–14.

Hodges JR, Davies RR, Xuereb JH, Casey B, Broe M, Bak TH, et al. Clinicopathological correlates in frontotemporal dementia. Ann Neurol 2004; 56: 399–406.

Josephs KA, Duffy JR. Apraxia of speech and nonfluent aphasia: a new clinical marker for corticobasal degeneration and progressive supranuclear palsy. Curr Opin Neurol 2008a; 21: 688–92.

Josephs KA, Duffy JR, Strand EA, Whitwell JL, Layton KF, Parisi JE, et al. Clinicopathological and imaging correlates of progressive aphasia and apraxia of speech. Brain 2006a; 129 (Pt 6): 1385–98.

Josephs KA, Petersen RC, Knopman DS, Boeve BF, Whitwell JL, Duffy JR, et al. Clinicopathologic analysis of frontotemporal and corticobasal degenerations and PSP. Neurology 2006b; 66: 41–8.

Josephs KA, Whitwell JL, Dickson DW, Boeve BF, Knopman DS, Petersen RC, et al. Voxel-based morphometry in autopsy proven PSP and CBD. Neurobiol Aging 2008b; 29: 280–9.

Josephs KA, Whitwell JL, Knopman DS, Boeve BF, Vemuri P, Senjem ML, Parisi JE, Ivnik RJ, Dickson DW, Petersen RC, Jack CR Jr. Two distinct subtypes of right temporal variant frontotemporal dementia. Neurology 2009; 3: 1443–50.

Josephs KA, Whitwell JL, Parisi JE, Petersen RC, Boeve BF, Jack CR Jr, et al. Caudate atrophy on MRI is a characteristic feature of FTLD-FUS. Eur J Neurol 2010; 17: 969–75.

Kelley BJ, Haidar W, Boeve BF, Baker M, Graff-Radford NR, Krefft T, et al. Prominent phenotypic variability associated with mutations in Progranulin. Neurobiol Aging 2009; 30: 739–51.

Kelley BJ, Haidar W, Boeve BF, Baker M, Shiung M, Knopman DS, et al. Alzheimer disease-like phenotype associated with the c.154delA mutation in progranulin. Arch Neurol 2010; 67: 171–7.

Downloaded from https://academic.oup.com/brain/article/134/9/2565/419546 by guest on 23 April 2025

Kertesz A. Frontotemporal dementia, Pick's disease. Ideggyogy Sz 2010; 63: 4–12.

Kertesz A, McMonagle P, Blair M, Davidson W, Munoz DG. The evolution and pathology of frontotemporal dementia. Brain 2005; 128 (Pt 9): 1996–2005.

Lashley T, Holton JL, Gray E, Kirkham K, O'Sullivan SS, Hilbig A, et al. Cortical alpha-synuclein load is associated with amyloid-beta plaque burden in a subset of Parkinson's disease patients. Acta Neuropathol 2008; 115: 417–25.

Lashley T, Rohrer JD, Bandopadhyay R, Fry C, Ahmed Z, Isaacs AM, et al. A comparative clinical, pathological and biochemical study of FUS proteinopathies. Brain 2011, in press.

Ling H, O'Sullivan SS, Holton JL, Revesz T, Massey LA, Williams DR, et al. Does corticobasal degeneration exist? A clinicopathological re-evaluation. Brain 2010; 133 (Pt 7): 2045–57.

Litvan I, Agid Y, Calne D, Campbell G, Dubois B, Duvoisin RC, et al. Clinical research criteria for the diagnosis of progressive supranuclear palsy (Steele-Richardson-Olszewski syndrome): report of the NINDS-SPSP international workshop. Neurology 1996; 47: 1–9.

Lladó A, Sánchez-Valle R, Rey MJ, Ezquerra M, Tolosa E, Ferrer I, Molinuevo JL. Catalan collaborative Study Group for FTLD. Clinicopathological and genetic correlates of frontotemporal lobar degeneration and corticobasal degeneration. J Neurol 2008; 255: 488–94.

Mackenzie IR, Baborie A, Pickering-Brown S, Du Plessis D, Jaros E, Perry RH, et al. Heterogeneity of ubiquitin pathology in frontotemporal lobar degeneration: classification and relation to clinical phenotype. Acta Neuropathol 2006; 112: 539–49.

Mackenzie IR, Neumann M, Bigio EH, Cairns NJ, Alafuzoff I, Kril J, et al. Nomenclature for neuropathologic subtypes of frontotemporal lobar degeneration: consensus recommendations. Acta Neuropathol 2009; 117: 15–8.

Mackenzie IR, Neumann M, Bigio EH, Cairns NJ, Alafuzoff I, Kril J, et al. Nomenclature and nosology for neuropathologic subtypes of frontotemporal lobar degeneration: an update. Acta Neuropathol 2010; 119: 1–4.

Mackenzie IR, Neumann M, Baborie A, Sampathu DM, Du Plessis D, Jaros E, et al. A harmonized classification system for FTLD-TDP pathology. Acta Neuropathol 2011. Advance Access published on June 5, 2011, doi: 10.1007/s00401-011-0845-8.

Mesulam MM. Slowly progressive aphasia without generalized dementia. Ann Neurol 1982; 11: 592–8.

Mesulam M, Wicklund A, Johnson N, Rogalski E, Léger GC, Rademaker A, et al. Alzheimer and frontotemporal pathology in subsets of primary progressive aphasia. Ann Neurol 2008; 63: 709–19.

Munoz DG, Neumann M, Kusaka H, Yokota O, Ishihara K, Terada S, et al. FUS pathology in basophilic inclusion body disease. Acta Neuropathol 2009; 118: 617–27.

Murray R, Neumann M, Forman MS, Farmer J, Massimo L, Rice A, et al. Cognitive and motor assessment in autopsy-proven corticobasal degeneration. Neurology 2007; 68: 1274–83.

Neary D, Snowden JS, Gustafson L, Passant U, Stuss D, Black S, et al. Frontotemporal lobar degeneration: a consensus on clinical diagnostic criteria. Neurology 1998; 51: 1546–54.

Neumann M, Rademakers R, Roeber S, Baker M, Kretzschmar HA, Mackenzie IR. A new subtype of frontotemporal lobar degeneration with FUS pathology. Brain 2009a; 132: 2922–31.

Neumann M, Roeber S, Kretzschmar HA, Rademakers R, Baker M, Mackenzie IR. Abundant FUS-immunoreactive pathology in neuronal intermediate filament inclusion disease. Acta Neuropathol 2009b; 118: 605–16.

Olichney J, Hansen L, Galasko D, Saitoh T, Hofstetter C, Katzman R, et al. The apolipoprotein e4 allele is associated with increased neuritic plaques and cerebral amyloid angiopathy in Alzheimer's disease and Lewy body variant. Neurology 1996; 47: 190–196.

Omar R, Sampson EL, Loy CT, Mummery CJ, Fox NC, Rossor MN, et al. Delusions in frontotemporal lobar degeneration. J Neurol 2009; 256: 600–7.

Pereira JM, Williams GB, Acosta-Cabronero J, Pengas G, Spillantini MG, Xuereb JH, et al. Atrophy patterns in histologic vs clinical groupings of frontotemporal lobar degeneration. Neurology 2009; 72: 1653–60.

Pick A. Uber die Beziehungen der senilen Hirnatrophie zur Aphasie. Prag Med Wochenschr 1892; 17: 165–7.

Piguet O, Halliday GM, Reid WG, Casey B, Carman R, Huang Y, et al. Clinical phenotypes in autopsy-confirmed Pick disease. Neurology 2011; 76: 253–9.

Rademakers R, Eriksen JL, Baker M, Robinson T, Ahmed Z, Lincoln SJ, et al. Common variation in the miR-659 binding-site of GRN is a major risk factor for TDP-43-positive frontotemporal dementia. Hum Mol Genet 2008; 17: 3631–42.

Rogalski E, Cobia D, Harrison TM, Wieneke C, Weintraub S, Mesulam MM. Progression of language decline and cortical atrophy in subtypes of primary progressive aphasia. Neurology 2011; 76: 1804–10.

Rohrer JD, Crutch SJ, Warrington EK, Warren JD. Progranulin-associated primary progressive aphasia: a distinct phenotype? Neuropsychologia 2010a; 48: 288–97.

Rohrer JD, Geser F, Zhou J, Gennatas ED, Sidhu M, Trojanowski JQ, et al. TDP-43 subtypes are associated with distinct atrophy patterns in frontotemporal dementia. Neurology 2010b; 75: 2204–11.

Rohrer JD, Guerreiro R, Vandrovcova J, Uphill J, Reiman D, Beck J, et al. The heritability and genetics of frontotemporal lobar degeneration. Neurology 2009; 73: 1451–6.

Rohrer JD, Lashley T, Holton J, Revesz T, Urwin H, Isaacs AM, et al. The clinical and neuroanatomical phenotype of FUS associated frontotemporal lobar degeneration. J Neurol Neurosurg Psychiatry 2010c; Advance Access published on July 16, 2010; doi:10.1136/jnnp.2010.214437.

Rohrer JD, Ridgway GR, Crutch SJ, Hailstone J, Goll JC, Clarkson MJ, et al. Progressive logopenic/phonological aphasia: erosion of the language network. Neuroimage 2010d; 49: 984–93.

Rohrer JD, Ridgway GR, Modat M, Ourselin S, Mead S, Fox NC, et al. Distinct profiles of brain atrophy in frontotemporal lobar degeneration caused by progranulin and tau mutations. Neuroimage 2010e; 53: 1070–6.

Rollinson S, Rohrer JD, van der Zee J, Sleegers K, Mead S, Engelborghs S, et al. No association of PGRN 3'UTR rs5848 in frontotemporal lobar degeneration. Neurobiol Aging 2011; 32: 754–5.

Sampathu DM, Neumann M, Kwong LK, Chou TT, Micsenyi M, Truax A, et al. Pathological heterogeneity of frontotemporal lobar degeneration with ubiquitin-positive inclusions delineated by ubiquitin immunohistochemistry and novel monoclonal antibodies. Am J Pathol 2006; 169: 1343–52.

Sánchez-Valle R, Forman MS, Miller BL, Gorno-Tempini ML. From progressive nonfluent aphasia to corticobasal syndrome: a case report of corticobasal degeneration. Neurocase 2006; 12: 355–9.

Saur D, Kreher BW, Schnell S, Kümmerer D, Kellmeyer P, Vry MS, et al. Ventral and dorsal pathways for language. Proc Natl Acad Sci USA 2008; 105: 18035–40.

Seelaar H, Rohrer JD, Pijnenburg YA, Fox NC, van Swieten JC. Clinical, genetic and pathological heterogeneity of frontotemporal dementia: a review. J Neurol Neurosurg Psychiatry 2011; 82: 476–86.

Seeley WW. Selective functional, regional, and neuronal vulnerability in frontotemporal dementia. Curr Opin Neurol 2008; 21: 701–7.

Seeley WW, Allman JM, Carlin DA, Crawford RK, Macedo MN, Greicius MD, et al. Divergent social functioning in behavioural variant frontotemporal dementia and Alzheimer disease: reciprocal networks and neuronal evolution. Alzheimer Dis Assoc Disord 2007; 21: S50–7.

Seeley WW, Carlin DA, Allman JM, Macedo MN, Bush C, Miller BL, et al. Early frontotemporal dementia targets neurons unique to apes and humans. Ann Neurol 2006; 60: 660–7.

Seeley WW, Crawford R, Rascovsky K, Kramer JH, Weiner M, Miller BL, et al. Frontal paralimbic network atrophy in very mild behavioural variant frontotemporal dementia. Arch Neurol 2008; 65: 249–55.

Downloaded from https://academic.oup.com/brain/article/134/9/2565/419546 by guest on 23 April 2025

Seeley WW, Crawford RK, Zhou J, Miller BL, Greicius MD. Neurodegenerative diseases target large-scale human brain networks. Neuron 2009; 62: 42–52.

Sergeant N, Wattez A, Delacourte A. Neurofibrillary degeneration in progressive supranuclear palsy and corticobasal degeneration: tau pathologies with exclusively "exon 10" isoforms. J Neurochem 1999; 72: 1243–9.

Shi J, Shaw CL, Du Plessis D, Richardson AM, Bailey KL, Julien C, et al. Histopathological changes underlying frontotemporal lobar degeneration with clinicopathological correlation. Acta Neuropathol 2005; 110: 501–12.

Snowden J, Neary D, Mann D. Frontotemporal lobar degeneration: clinical and pathological relationships. Acta Neuropathol 2007; 114: 31–8.

Sporns O, Zwi JD. The small world of the cerebral cortex. Neuroinformatics 2004; 2: 145–62.

Tang-Wai DF, Josephs KA, Boeve BF, Dickson DW, Parisi JE, Petersen RC. Pathologically confirmed corticobasal degeneration presenting with visuospatial dysfunction. Neurology 2003; 61: 1134–5.

Urwin H, Josephs KA, Rohrer JD, Mackenzie IR, Neumann M, Authier A, et al. FUS pathology defines the majority of tau- and TDP-43-negative frontotemporal lobar degeneration. Acta Neuropathol 2010; 120: 33–41.

Vanvoorst WA, Greenaway MC, Boeve BF, Ivnik RJ, Parisi JE, Eric Ahlskog J, et al. Neuropsychological findings in clinically atypical autopsy confirmed corticobasal degeneration and progressive supranuclear palsy. Parkinsonism Relat Disord 2008; 14: 376–8.

Wakana S, Jiang H, Nagae-Poetscher LM, van Zijl PC, Mori S. Fiber tract-based atlas of human white matter anatomy. Radiology 2004; 230: 77–87.

Weintraub S, Mesulam M. With or without FUS, it is the anatomy that dictates the dementia phenotype. Brain 2009; 132 (Pt 11): 2906–8.

Whitwell JL, Jack CR Jr, Boeve BF, Senjem ML, Baker M, Ivnik RJ, et al. Atrophy patterns in IVS10 + 16, IVS10 + 3, N279K, S305N, P301L, and V337M MAPT mutations. Neurology 2009a; 73: 1058–65.

Whitwell JL, Przybelski SA, Weigand SD, Ivnik RJ, Vemuri P, Gunter JL, et al. Distinct anatomical subtypes of the behavioural variant of frontotemporal dementia: a cluster analysis study. Brain 2009b; 132 (Pt 11): 2932–46.

Whitwell JL, Jack CR Jr, Senjem ML, Parisi JE, Boeve BF, Knopman DS, et al. MRI correlates of protein deposition and disease severity in postmortem frontotemporal lobar degeneration. Neurodegen Dis 2009c; 6: 106–17.

Whitwell JL, Jack CR Jr, Parisi JE, Knopman DS, Boeve BF, Petersen RC, et al. Imaging signatures of molecular pathology in behavioral variant frontotemporal dementia. J Mol Neurosci 2011. Advance Access published on May 10, 2011; doi:10.1007/s12031-011-9533-3.

Williams DR, Holton JL, Strand C, Pittman A, de Silva R, Lees AJ, et al. Pathological tau burden and distribution distinguishes progressive supranuclear palsy-parkinsonism from Richardson's syndrome. Brain 2007; 130 (Pt 6): 1566–76.

Winklhofer KF, Tatzelt J, Haass C. The two faces of protein misfolding: gain- and loss-of-function in neurodegenerative diseases. EMBO J 2008; 27: 336–49.

Yokota O, Tsuchiya K, Arai T, Yagishita S, Matsubara O, Mochizuki A, et al. Clinicopathological characterization of Pick's disease versus frontotemporal lobar degeneration with ubiquitin/TDP-43-positive inclusions. Acta Neuropathol 2009; 117: 429–44.

Zhou J, Greicius MD, Gennatas ED, Growdon ME, Jang JY, Rabinovici GD, et al. Divergent network connectivity changes in behavioural variant frontotemporal dementia and Alzheimer's disease. Brain 2010; 133 (Pt 5): 1352–67.

Downloaded from https://academic.oup.com/brain/article/134/9/2565/419546 by guest on 23 April 2025